Tunnels vs. Wires: A Comparative Analysis of Two 3D Steering Tasks in Virtual Environments

Mohammadreza Amini
Concordia University
Montreal, QC, Canada
mohammadreza.amini@concordia.ca

Wolfgang Stuerzlinger
SIAT, Simon Fraser University
Vancouver, BC, Canada
w.s@sfu.ca

Shota Yamanaka
LY Corporation
Chiyoda-ku, Tokyo, Japan
syamanak@lycorp.co.jp

Hai-Ning Liang
The Hong Kong University of Science and Technology (Guangzhou)
Guangzhou, Guangdong, China
hainingliang@hkust-gz.edu.cn

Anil Ufuk Batmaz
Concordia University
Montreal, QC, Canada
ufuk.batmaz@concordia.ca

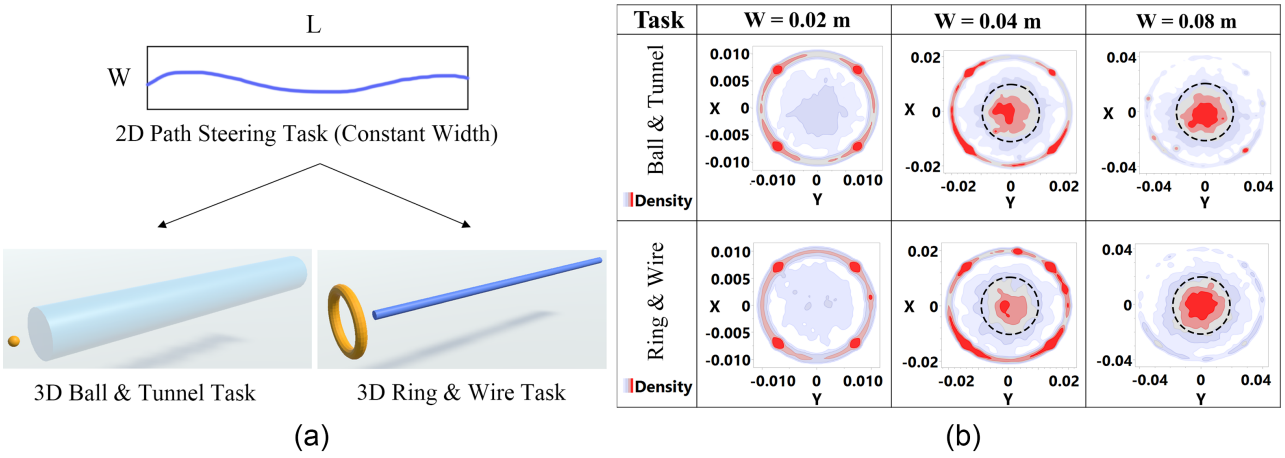

Figure 1: (a) Visual representation of 2D steering through a path with constant width, and the two 3D steering tasks investigated in this study, i.e., Ball-and-Tunnel and Ring-and-Wire. (b) Heatmaps showing the 2D density of track point spread in each path width condition for both 3D steering tasks. Dashed circles outline the smaller path width inside the larger one as a reference.

Abstract

Steering involves continuous movement along constrained paths, well-studied in 2D. The extensions to 3D using the Ring-and-Wire and Ball-and-Tunnel tasks were often treated as interchangeable in previous work. In this paper, we directly compare these two tasks through a within-subjects user study (n = 18) with varying 3D path orientations. The results show that Ring-and-Wire significantly outperformed Ball-and-Tunnel, with 17.17% lower task time, 21.65% higher throughput, and 21.52% faster average speed. Participants also preferred Ring-and-Wire and reported lower workload. Visual ambiguity, especially near the tunnel's rear surface, complicated spatial perception in the Ball-and-Tunnel task. We thus recommend that future studies choose 3D steering tasks carefully for experiments, as the two tasks are not interchangeable.

VRST '25, Montreal, QC, Canada

ACM ISBN 979-8-4007-2118-2/2025/11
https://doi.org/10.1145/3756884.3766023

CCS Concepts

• **Human-centered computing** → **HCI design and evaluation methods**; **Virtual reality**; **Mixed / augmented reality**.

Keywords

Steering Law, Virtual Reality, Trajectory-based Interactions

ACM Reference Format:
Mohammadreza Amini, Wolfgang Stuerzlinger, Shota Yamanaka, Hai-Ning Liang, and Anil Ufuk Batmaz. 2025. Tunnels vs. Wires: A Comparative Analysis of Two 3D Steering Tasks in Virtual Environments. In *31st ACM Symposium on Virtual Reality Software and Technology (VRST '25), November 12–14, 2025, Montreal, QC, Canada.* ACM, New York, NY, USA, 11 pages. https://doi.org/10.1145/3756884.3766023

1 Introduction

Steering is an interaction method in Human-Computer Interaction (HCI), involving continuous movement along a constrained path [1]. With its growing use in interfaces, such as nested menus, drawing, and path-following, research has increasingly focused on modeling steering behaviors [1]. These models enhance our understanding of

human motor control, guide the design of novel interfaces [25, 41], and support the evaluation of interaction techniques [2, 25].

The *Steering law*, a mathematical model for predicting *Movement Time* (MT) in steering tasks [1], is one of the widely studied models for steering behavior in HCI [45]. Many studies have extended the law to improve its accuracy in 2D interfaces [3, 48, 50]. More recently, researchers have begun exploring its applicability in 3D Extended Reality (XR) [44, 45, 51], investigating how spatial constraints and interaction modalities influence steering behavior in immersive settings. While, the 2D representation of constrained paths for steering is relatively straightforward (e.g., Figure 1-a), extending this task to XR introduces new challenges, such as the increased degrees of freedom [28], limited visual depth cues [28, 44], varying path orientations [28], and the lack of physical support [44]. These complexities have led to the development of diverse steering law experiments. As steering interactions become more common in XR environments, it is necessary to examine how methodological decisions, specifically task type, affect user performance and experience. Experimental clarification of these differences is essential for establishing well-grounded evaluation methodologies.

Zhai et al. [53] originally proposed the *Ring-and-Wire* (or Buzz Wire) task as the 3D steering task, where users guide a ring along a wire. This task has been applied in domains such as eye-hand coordination [32], fine motor skill rehabilitation [13, 14], and 3D mid-air interaction [17]. Yet, this task has been largely ignored in 3D Steering law studies. Instead, the *Ball-and-Tunnel* task, i.e., pushing a target ball inside a semi-transparent tunnel of constant width, has become more common, often justified by the added rotational complexity of Ring-and-Wire [28, 44]. Despite both being mid-air manipulation tasks and frequently cited together, it remains unclear whether they are interchangeable or whether differences in task dynamics limit the transferability of findings across them.

To explore this, we conducted a user study comparing these two tasks across many 3D directions, constraining ring rotation in Ring-and-Wire to isolate translational movement and enable direct comparison with Ball-and-Tunnel. By comparing these conceptually similar but structurally distinct tasks, our goal is to provide a comprehensive understanding that guides their future use in 3D steering studies and the design of practical XR applications.

In short, this work's main contributions are: **(1.)** We empirically validated the applicability of the Steering law for a modified Ring-and-Wire task. **(2.)** We revealed that the Ring-and-Wire and Ball-and-Tunnel tasks are not interchangeable. **(3.)** We demonstrated that the Ball-and-Tunnel task imposes a higher workload and challenges participants' perception of the path boundaries. **(4.)** Building on these findings, we suggest practical implications for future Steering law studies.

2 Related Work

2.1 Steering Law

Modeling human motor behavior is an important research topic in HCI and aims to better understand, predict, and optimize interaction [33, 53]. Despite its complexity, human motor performance, e.g., in pointing [5, 16] or navigation [1, 3], is well-modeled by mathematical models widely used in HCI for both 2D and 3D environments [33, 45, 53]. Accot and Zhai's *Steering law* [1] for trajectory movements, e.g., path steering or goal-crossing [4], is widely studied and applied in HCI research [25, 36, 53]. As presented in Equation 1, the Steering law predicts Movement Time (MT), i.e., the total time to traverse a bounded path (C), by dividing the path into infinitesimal sections with length ds and width $W(s)$.

$$MT = a + b \int_C \frac{ds}{W(s)} \tag{1}$$

For steering through constrained paths with constant width (shown in Figure 1-a), e.g., navigating through menus or scroll bars with fixed width, Equation 1 simplifies to Equation 2 [1]. Based on Equation 2, the Index of Difficulty (ID) for the steering task is defined as the ratio of path length (L) to its width (W), resulting in a unitless measure that reflects the difficulty of the steering task [1, 4].

$$MT = a + b \cdot ID,\ ID = \frac{L}{W} \tag{2}$$

As the task difficulty increases, MT tends to rise, a relationship captured by a performance metric called Throughput (Equation 3), commonly used to evaluate the performance of steering tasks [2, 46]. As ID is a unitless measure, throughput (TP) is expressed in inverse seconds (s^{-1}) [2, 25]. Recently, Kasahara et al. [25] suggested the effective width ($W_e = 4.133 \times SD$, SD is the standard deviation perpendicular to the direction of the movement) for the calculation of TP to stabilize it across varying speed-accuracy biases [25].

$$TP = \frac{ID}{MT} \tag{3}$$

The Steering law has been widely used to design and evaluate interaction techniques and input devices [2, 25, 41]. It is also the foundation for many HCI studies aiming to extend the understanding of human steering performance in more complex scenarios, e.g., the effect of the Control-Display ratio [3], steering through corners [36], the negative influence of latency [48], or navigating through consecutive paths with different sizes [49].

2.2 Steering Tasks in 3D Environments

With the growth of immersive technologies, such as Head-Mounted-Displays (HMD), the Steering law has been applied in a variety of 3D scenarios, ranging from direct object manipulation to locomotion tasks, e.g., virtual driving [51, 53] or drone piloting [23]. Zhai et al., in their early efforts to extend the Steering law beyond 2D interfaces [53], suggested the *Ring-and-Wire* task for 3D VR studies, owing to its emerging applications in HCI research [7, 39]. In this task, participants use a ring to navigate along a wire, avoiding contact between them. This task has been widely adopted in 3D interaction studies as a well-established motor control task [13, 37] that requires continuous movement along the path, allows for clear performance assessment [14, 31] with progressive adjustment of task difficulty [31, 37] and isolates steering performance [17, 26, 35].

Christou et al. [13] evaluated a Ring-and-Wire task in VR, finding it a promising tool for stroke rehabilitation. Lui et al. [31] used this task to compare adaptive and fixed immersive VR training, showing its effectiveness for fine motor skill training. Similarly, Radhakrishnan et al. [37] investigated the application of VR for motor skill training and its relationship to physiological arousal. Mariani et al. [35] implemented a VR-based Ring-and-Wire task,

as a part of an adaptive training system for robot-assisted surgery, resulting in improved users' surgical motor skills. This task is also used as a performance evaluation tool, e.g., Lee et al. [26] validated a VR robotic simulator by comparing user performance on four tasks, including Ring-and-Wire. Also, Gemici et al. [17] used this task to evaluate how Signed Distance Fields (SDF) can dynamically control object speed during distant 3D mid-air manipulation. However, despite its frequent use, the Ring-and-Wire task has not been studied in the context of the 3D Steering law. Also, despite its frequent use in real-world and XR applications, the Ring-and-Wire task was only suggested by Accot and Zhai [53] or mentioned as a conceptual example of steering interaction [12], but has not been critically examined in 3D XR steering studies. Instead, the *Ball-and-Tunnel* task, i.e., navigating a target ball inside a semi-transparent tunnel [28], has been used in the literature for such investigations.

Liu et al. [28] studied the effect of path curvature and orientation in 3D space and showed that the Steering law (Equation 2) provides a good description for 3D steering tasks. Yet, they proposed the Ball-and-Tunnel task as a more "*straightforward*" alternative to the Ring-and-Wire task [28]. This choice was further justified in other studies [28, 30, 44] by noting that the Ring-and-Wire task introduces additional complexity owing to the rotation of the ring relative to the wire, which can dynamically change the available lateral movement freedom, and thus task difficulty. In contrast, the Ball-and-Tunnel task isolates translational movement in a constant-width path. Following this trend, Wei et al. [44] used a Ball-and-Tunnel task and empirically proposed a refined Steering law model accounting for the effect of frame rate in XR. Similarly, Wei et al. [45] implemented this task to study the effect of movement direction on 3D mid-air steering performance. Finally, Liu et al. [30] extended the Steering law to 3D interactions with force feedback, using a Ball-and-Tunnel task with added haptic feedback.

3 Motivation and Research Questions

When the rotational movement in the Ring-and-Wire task is constrained to remain orthogonal to the wire, both Ring-and-Wire and Ball-and-Tunnel tasks can be conceptually framed as steering through a constant-width path [28, 44]. Liu et al. justified Ball-and-Tunnel to "limit the complexity" in steering tasks and proposed it as an "alternative interaction task" [28]. Drawing from prior work that frames the Steering law as a series of goal-crossing tasks [1, 4], the ring can be interpreted as a moving slice of the tunnel, effectively reversing the motion while preserving the structure.

This conceptual overlap has led to the assumption that the two are interchangeable in 3D steering studies. As a result, the 3D steering literature is built upon both tasks, treating them as functionally equivalent and using them interchangeably to model, evaluate, and compare user performance. However, this assumption lacks empirical validation. Given the growing number of 3D steering studies, it is essential to examine whether task type affects behavior and whether results across studies using different tasks are comparable, motivating the following Research Questions (RQs): (*RQ1.*) Are the Ring-and-Wire and Ball-and-Tunnel tasks interchangeable for studying 3D steering? If not, (*RQ2.*) what are the key differences between these tasks in the context of 3D mid-air interaction?

Previous studies have shown that motor performance in VR is influenced by the complex characteristics of mid-air interactions, e.g., the presence of stereo viewing [8], the vergence-accommodation conflict [11], depth perception issues [28, 44], and increased degrees of freedom in movement and control [28, 45]. Factors like the experimental task itself [5] and its visual complexity [38] can also affect 3D interactions. Based on these insights, we hypothesize that: (**H1.**) *The Ring-and-Wire task offers higher motor performance, in terms of shorter steering time, fewer boundary hits, higher throughput, and narrower traversed path, compared to the Ball-and-Tunnel task.* (**H2.**) *The Ball-and-Tunnel task induces higher cognitive load and has lower usability, compared to the Ring-and-Wire.*

4 User Study

Pilot Studies: Before the main study, we ran three small pilots (n=6) to calibrate task design. Pilot 1 compared path placement at the dominant shoulder, non-dominant shoulder, and chest with W=4 cm, L=20 cm, identifying chest placement as most comfortable. Pilot 2 tested path lengths of 35–45 cm, selecting 40 cm as the maximum L reachable in a seated position (similar to anthropometric data [40]). Pilot 3 used the finalized conditions to estimate effect sizes for G*Power [15] and explore performance trends.

Participants: Based on the results of Pilot 3, we calculated the minimum sample size needed for RM ANOVA using G*Power [15] with $\alpha = .05$, statistical power set to 0.95, and a large effect size ($\eta^2 = .14$). Thus, we recruited 18 participants (9 female, 9 male), aged between 22 and 32 years ($M = 25.89$, $SD = 2.85$). They were volunteers recruited from the university campus and the general public through online flyers. All but one were right-handed, and all had normal or corrected-to-normal vision.

Apparatus: We used an Intel(R) i7-12700F processor at 2.1 GHz, 16 GB RAM, an NVIDIA GeForce RTX 3060 Ti graphics card, and a Meta Quest 3 as the VR HMD. The virtual models were designed using Blender 4.2, and the VR system was implemented using Unity 2022.3.49f1 with Meta XR All-in-One SDK 68.0.1.

Procedure: Each session began with a consent form, demographics survey, and a study overview. After wearing the headset, the participants completed training trials (<5 min), in VR and then proceeded to the main experiment. Following previous studies [1, 9, 44, 48], participants remained seated and were instructed to perform each task as fast and as accurately as possible, using virtual hand interaction [45] with their dominant hand. Based on the outcome of pilot 1, all path conditions were centered around a fixed point, i.e., 15 cm below and 35 cm in front of the headset, to keep the visual size of objects consistent across participants.

In the main study, participants clicked a start button while facing forward to initiate the experiment and calibrate scene placement. Trials were presented sequentially. In each trial, participants had to grab the moving target—the ring or the ball—positioned 2.5 cm before the path's starting point, and steer it along the path to the end (see Figure 1-a, lower row). To reduce visual complexity and isolate spatial constraints, the virtual hand was invisible during steering. If participants collided with the path boundaries, a short error sound provided auditory feedback. While contact persisted, the path turned red to offer continuous visual feedback. If the object

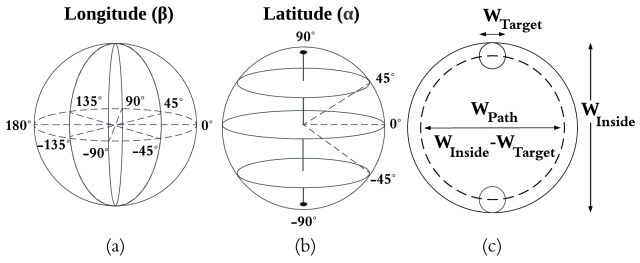

Figure 2: Longitude [28] (a) and Latitude [28] (b) values considered in our experimental design as path endpoints. (c) Definition of the path width (W_{Path}) based on the target width (W_{Target}) and inner diameter of the path (W_{Inside}).

was pushed completely out of the path, the trial was reset. Upon completion, a short success sound signalled the end of the trial.

Participants were reminded throughout the experiment to balance speed and accuracy, and encouraged to take breaks to reduce fatigue, preventing the gorilla arm effect [21]. The experimenter monitored performance and prompted breaks when signs of fatigue, e.g., performance decline, were observed. On average, participants took 3.5 breaks (SD = 1.33), each lasting between 5 and 12 minutes. After the main experiment, participants completed a post-experiment questionnaire, including subjective feedback, the System Usability Score (SUS) [24], and the perceived workload (NASA-TLX) [22] (included in the supplementary material). Each user study session lasted under 45 minutes.

Experimental Design: We used a within-subjects design with two tasks as explained below:

Ball & Tunnel (BT) Task: As in previous studies [28–30, 44], this task involves a semi-transparent tunnel and a target ball (Figure 1-a). Unlike previous work [28, 30], the target ball can be freely manipulated inside the tunnel rather than being restricted solely to forward movements, to align with practical applications and with the 2D steering task that 3D research seeks to extend [1, 3, 48].

Ring & Wire (RW) Task: This task uses a ring and a wire, following the common RW design (Figure 1-a). Participants grab the ring and steer it along the wire. To isolate translational movement and eliminate the rotational complexity associated with this task [28, 30, 44], the ring's orientation is fixed to remain perpendicular to the wire. This also aligns with BT, where the sphere lacks visible rotation. Allowing the ring to tilt would distort the effective path width, making direct comparison unfair. Constraining the ring's rotation ensures a more meaningful comparison of controlled movement along paths with consistent width.

Based on prior work [28, 44, 45], we selected a common range of path lengths and widths for 3D mid-air steering studies, see below. To ensure the paths were comfortably reachable, we referred to anthropometric data [40, 52] and pilot 2 to confirm that the selected parameters were practical, comfortable, and provided easily perceivable task boundaries for seated participants in the virtual environment. To capture the effects of movement direction in 3D mid-air interactions [28, 45], we included path orientations aligned with the main axes and all 45°diagonals. To control for handedness effects [28], each orientation included both movements (left-to-right and right-to-left), resulting in 26 distinct path orientations. The independent variables are summarized below:

Task Type: Ball & Tunnel (BT), Ring & Wire (RW)
Path Width (W): 0.02, 0.04, 0.08 m
Path Length (L): 0.2, 0.4 m
3D Path Orientations (R0-R25): 6 principal axes, 12 face diagonals, 8 space (corner) diagonals.

As shown in Figure 2(c), W is the lateral movement constraint. Following prior work [28, 29, 44], W is calculated as the inner diameter of the ring or tunnel minus the diameter of the target (i.e., the wire or ball), which was fixed at 1 cm across all conditions. We counterbalanced the conditions across participants by randomizing path 3D orientation sequences for each participant and applying a Latin Square design to the other independent variables. Two path Lengths (L) and three path widths (W) resulted in 4 unique ID levels (IDs = 2.5, 5.0, 10.0, 20.0). Each participant performed 3 $W \times 2$ $L \times 26$ *Orientations* $\times 2$ *Tasks* $\times 2$ *repetitions* = 624 *trials*.

We recorded task execution time (s), effective throughput (s^{-1}), and average speed (m/s) for each trial. Because boundary contact was allowed, we measured both the number of collisions and error time (duration of contact). This separation distinguishes pure steering time (error-free movement) from error time, enabling finer analysis of control behavior. Additionally, for each frame, we captured the relative position of the wire (or ball) within the ring (or tunnel) using local axes perpendicular to the movement direction. From this, we computed the standard deviation of the traversed path from the mean trajectory (SD_{xy}) and from the path centerline (CSD_{xy}).

5 Results

Except for the subjective measures, we conducted Repeated Measures ANOVA ($\alpha = .05$) to examine main effects and interactions, applying Bonferroni corrections for post-hoc comparisons. Log transformations were used for non-normal data (Skewness and Kurtosis beyond ±1.0 [10, 18]), and Greenhouse–Geisser corrections were applied when sphericity was violated. Analyses were performed in IBM SPSS Statistics 30.0.

5.1 Steering Time

RM ANOVA revealed a significant main effect of the task, path length, and width on task completion time, see Table 1 for the statistics. Participants executed RW (M = 433.33 ms, SD = 302.06) in significantly less time than BT (M = 523.20 ms, SD = 401.30), shown in Figure 3(a). Pure steering time follows a similar trend with BT resulting in higher times (M = 406.68 ms, SD = 351.46), compared to RW (M = 323.50 ms, SD = 287.53), as presented in Figure 3(b). A significant interaction was observed between length and width, suggesting that the impact of width varied depending on the path length. However, no significant interactions were found between task and length, or task and width. Pairwise comparisons revealed a significantly higher completion time for BT compared to RW in all width and length conditions (Figure 4 a-b).

For task completion time across different path 3D orientations, RM ANOVA identified a significant main effect ($F(25, 425) = 7.06$, $p < .001$, $\eta^2 = .293$), suggesting that 3D orientation influenced task

completion time. However, no significant interaction between task type and rotation was observed ($F(8.50, 144.53) = 1.528$, $p = 0.148$, $\eta^2 = .082$), showing that the performance difference between task types was relatively stable across orientations. Besides, rotation exhibited notable non-linear influences on task execution time (polynomial contrast tests revealed significantly higher-order effects, e.g., cubic: $F(1, 17) = 4.00$, $p = .062$, 8th-order: $F(1, 17) = 46.70$, $p < .001$), suggesting that movement time varied irregularly across 3D orientations.

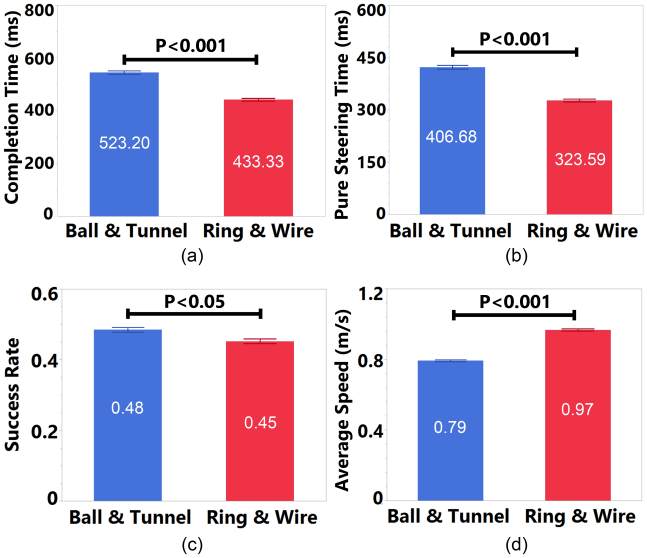

Figure 3: (a) Task completion time, (b) pure steering time, (c) success rate, and (d) average speed. (In this paper, error bars represent the standard error of the mean.)

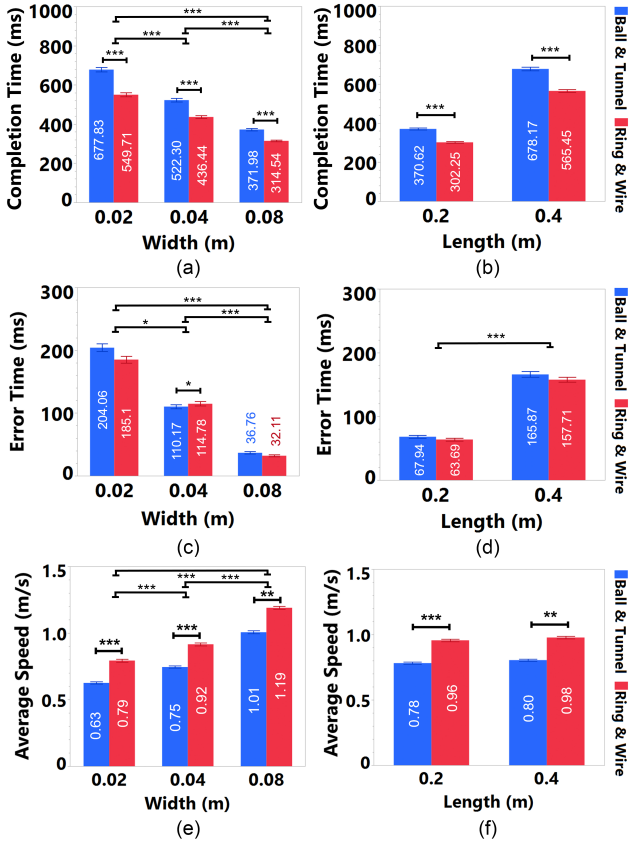

Figure 4: (a-b) Completion time, (c-d) error time, (e-f) average speed for width (left) and length (right). Significance levels are $p < .05$ (*), $p < .01$ (**) and $p < .001$ (***).

5.2 Hitting Boundaries

Success Rate. An RM ANOVA was conducted to compare success rates, i.e., the ratio of trials without hitting the boundaries. Participants were more successful in performing the task without hitting the boundaries in BT ($M = .485$, $SD = .067$) compared to RW ($M = .452$, $SD = .059$) ($F(1, 17) = 4.74$, $p < .044$, $\eta^2 = .218$). There was also a significant effect of width ($F(2, 34) = 61.68$, $p < .001$, $\eta^2 = .784$), indicating a higher success rate as path width increased. The task and width interaction was not significant ($F(2, 34) = 1.221$, $p = .307$, $\eta^2 = .067$), suggesting the performance difference between techniques remained relatively consistent across widths. Additional analysis on path orientations revealed a significant effect ($F(25, 425) = 2.901$, $p < .001$, $\eta^2 = .146$), as well as a significant interaction between task and orientation ($F(25, 425) = 1.981$, $p < .004$, $\eta^2 = .104$), suggesting that the effect of path 3D orientation on success rate depends on the task type.

Error Time. Significant main effects of path length and width (shown in Table 1 and Figure 4(c-d)) indicate that both spatial dimensions significantly affected total error time. Besides, significant interaction was observed between length and width, suggesting that the influence of width on error time varied depending on the path length across both task types. A significant main effect of 3D path orientation on error time was also observed ($F(10.36, 176.19) = 3.91$, $p < .001$, $\eta^2 = .187$).The Task × 3D path orientation interaction was also significant ($F(10.24, 174.02) = 2.33$, $p < .013$, $\eta^2 = .121$), suggesting that the pattern of error time across orientations differed between BT and RW.

5.3 Average Speed

As shown in Table 1 and Figure 3(d), participants were significantly faster in RW ($M = 0.96m/s$, $SD = 0.51$) than in BT ($M = 0.79m/s$, $SD = 0.42$). Pairwise comparisons showed that participants became significantly faster as width increased (Figure 4 e-f), with all width-level differences statistically significant. The interaction between width and length was also significant (Table 1). Further analysis of this interaction revealed that longer lengths significantly slowed performance only at the narrowest width (0.02 m, $p = .006$). This difference was no longer significant for wider target widths.There was a significant main effect of 3D path orientation ($F(25, 425) = 7.11$, $p < .001$, $\eta^2 = .30$) with a significant interaction between task and 3D orientation ($F(25, 425) = 1.68$, $p < .043$, $\eta^2 = .09$), indicating the effect of 3D orientation varied by task. The effect of

Table 1: Repeated-measures ANOVA results for task completion time, error time, and average speed, showing the main effects and interactions of Task Type (T), Width (W), and Length (L). Significant results are highlighted in gray.

	Task Completion Time			Error Time			Average Speed		
	Value	p	η_p^2	Value	p	η_p^2	Value	p	η_p^2
T	F(1, 17) = 28.859	**<.001**	.629	F(1, 17) = 0.419	.526	.024	F(1, 17) = 28.859	**<.001**	.629
L	F(1, 17) = 807.901	**<.001**	.979	F(1, 17) = 886.434	**<.001**	.981	F(1, 17) = 2.901	.107	.146
W	F(1.22, 20.74) = 50.889	**<.001**	.750	F(1.24, 21.12) = 80.48	**<.001**	.826	F(1.22, 20.741) = 50.889	**<.001**	.750
$T \times L$	F(1, 17) = 0.044	.836	.003	F(1, 17) = 0.004	.950	<.001	F(1, 17) = 0.044	.836	.003
$T \times W$	F(2, 34) = 0.608	.514	.035	F(1.45, 24.59) = 1.412	.257	.077	F(2, 34) = 0.608	.514	.035
$L \times W$	F(1.35, 22.90) = 5.239	**.023**	.236	F(1.24, 21.02) = 17.708	**<.001**	.510	F(1.35, 22.90) = 5.239	**.023**	.236
$T \times L \times W$	F(2, 34) = 0.162	.851	.009	F(1.28, 21.72) = 3.302	.074	.163	F(2, 34) = 0.162	.851	.009

orientation on the average speed was not linear, as indicated by the non-significant linear contrast ($F(1, 17) = 0.033$, $p = .858$).

5.4 Throughput and Model-Fit

The throughput for BT, $M = 13.12\ s^{-1}$ was significantly lower compared to RW, $M = 15.96\ s^{-1}$ ($F(1, 17) = 28.579$, $p < .001$, $\eta^2 = .63$) (Figure 5-a).

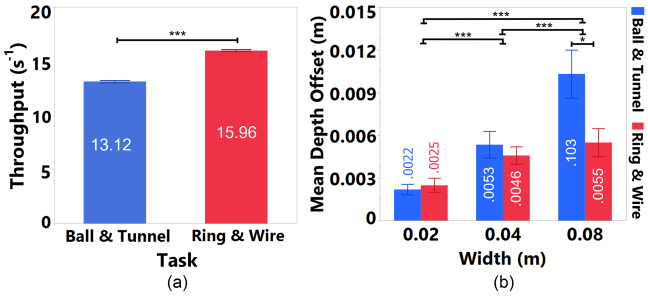

Figure 5: (a) Throughput for Ball-and-Tunnel and Ring-and-Wire. (b) Mean depth offset of steered tracks on the frontal plane. Significance levels are $p < .05$ (*) and $p < .001$ (***).

We conducted a linear regression using both pure steering time (movement within the path) and task completion time (movement within and on the boundaries). As different combinations of path length and width can yield identical ID values, this may limit the number of points for creating meaningful regressions. To improve results' generalizability, and following Gori et al.'s recommendations [20], we account for each individual combination of path length and width in our regression rather than relying solely on ID values. Execution time was regressed over the ID based on Equation 2 (Figure 6-a). Separate linear regressions for each task show that the task completion time can be modeled as $MT = 231.51 + 31.46 * ID$ ($R^2 = 0.96$, $Adj.R^2 = 0.94$) and $MT = 187.74 + 25.87 * ID$ ($R^2 = 0.97$, $Adj.R^2 = 0.96$) for BT and RW, respectively. These results indicate a strong fit to the Steering law in both tasks. A similarly strong fit was observed for pure steering time (Figure 6-b),

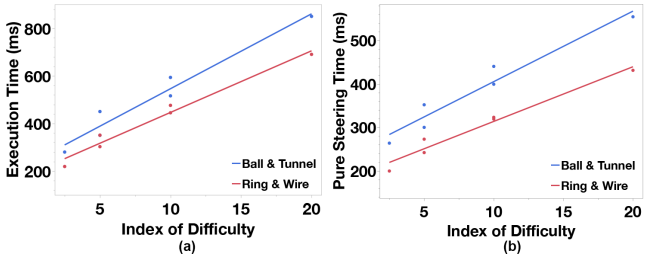

Figure 6: Steering law model fit for (a) task completion time and (b) pure steering time.

where $MT = 242.94 + 16.24 * ID$ (R^2 : 0.94, $Adj.R^2$: 0.93) for BT, and $MT = 187.80 + 12.59 * ID$ (R^2 : 0.96, $Adj.R^2$: 0.95) for RW.

5.5 Track Analysis

Standard Deviation. To analyze path spread relative to the movement center within the constrained area, we computed Wobbrock et al.'s 2D standard deviation (SD_{xy}) using [47].

A RM ANOVA on SD_{xy} across Width (Figure 7(a)) showed no significant effect on Task ($F(1, 17) = 0.19$, $p = .673$, $\eta^2 = .01$). However, Width had a significant effect ($F(1.12, 19.04) = 462.88$, $p < .001$, $\eta^2 = .98$), with SD_{xy} increasing as path width increased. The Task and Width interaction was not significant ($F(1.12, 18.96) = 2.08$, $p = .168$, $\eta^2 = .11$), showing that both tasks conform similarly to changes in W in terms of path spread.

To further examine movement density within the constrained paths, we analyzed the spatial distribution, i.e., where the ring intersected with the wire or the ball moved inside the tunnel at each frame. To visualize lateral movement density perpendicular to the direction of the movement in both tasks, we generated heatmaps of all recorded track points. As shown in Figure 1(b), a consistent pattern emerges: as path width increases, the movement shifts from the boundaries toward the center. Dashed reference circles (e.g., the 0.04 m circle inside the path $W = 0.08$ m) illustrate that steering becomes increasingly concentrated within the bounds of

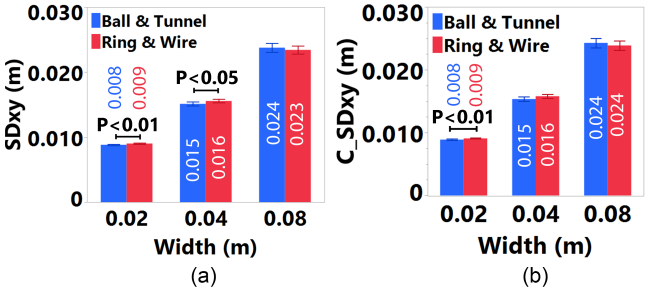

Figure 7: 2D Standard Deviation from the (a) center of the movement (SD_{xy}) and (b) center of the path (C_SD_{xy}).

the narrower path, highlighting a tendency toward centralization as spatial constraints loosen.

Standard Deviation from Center. By replacing mean recorded x and y values with 0 in SD_{xy}, we computed 2D standard deviation from the central line of the path (C_SD_{xy}) for each path width (Figure 7(b)). RM ANOVA results identified no significant differences for Task ($F(1, 17) = 0.07$, $p = .790$, $\eta^2 = .004$), indicating that overall track deviation from center did not differ between BT and RW. Yet, We found a significant effect on Width ($F(1.11, 18.88) = 564.06$, $p < .001$, $\eta^2 = .971$), with C_SD_{xy} increasing as path width increased. The interaction between Task and Width was not significant ($F(1.10, 18.70) = 1.92$, $p = .182$, $\eta^2 = .102$), showing that both tasks demonstrated comparable increases in deviation from the centerline at higher widths.

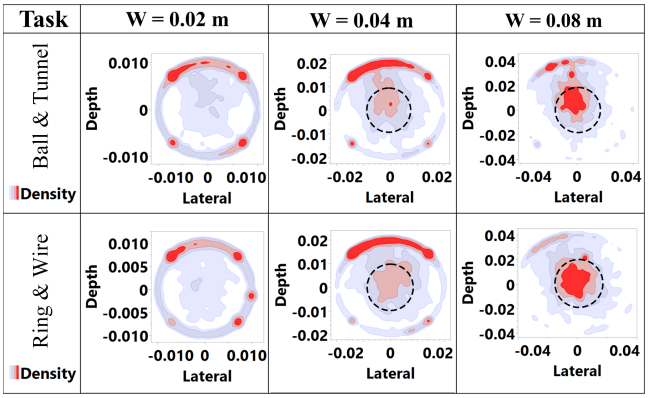

Figure 8: Heatmaps for steering only on the frontal plane in 3D space, showing the 2D density of track point spread for each path width condition in both steering tasks. Dashed circles outline the smaller path width inside the larger one as a reference.

Frontal Plane To examine depth movement variability, we isolated the 3D path orientations on the frontal plane, i.e., the plane perpendicular to the participant's viewing direction. By separating this frontal plane, we can map the local x and y axes of track points to the depth and lateral directions, respectively. Depth here refers to the extent of movement into 3D space, with positive values indicating a shift toward the rear of the tunnel or ring, and the lateral axis

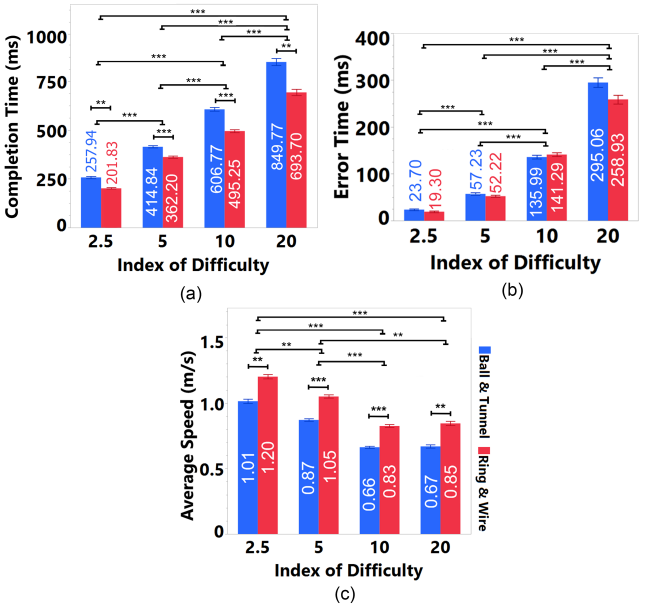

Figure 9: (a) Task completion time, (b) error time, (c) average speed for each task type across IDs. Significance levels are $p < .05$ (*), $p < .01$ (**) and $p < .001$ (***).

represents movement that is perpendicular to depth. This mapping enabled analysis of depth offsets in steered paths. As shown in the density heatmaps (Figure 8), track points increasingly shift in depth at the largest path width ($W = 0.08\ m$). A paired-sample t-test confirmed that BT had a significantly greater depth offset than RW at this width ($t(17) = 2.70$, $p = .015$, Cohen's d = 0.64, indicating deeper average paths (Figure 5(b)).

5.6 Index of Difficulty

Task Completion Time results revealed significant differences for task ($F(1, 17) = 22.18, p < .001, \eta^2 = .566$) and ID ($F(3, 15) = 103.30$, $p < .001, \eta^2 = .954$). The task and ID interaction was not significant. Pairwise comparisons showed significantly lower task completion times for RW across all IDs (shown in Figure 9 a).

Error Time results significantly increased with task difficulty ($F(1.41, 24.02) = 118.72$, $p < .001$, $\eta^2 = .875$). Bonferroni-corrected pairwise comparisons revealed significant differences in error time between IDs (shown in Figure 9 b).

Average Speed revealed significant differences for task ($F(1, 17) = 22.57$, $p < .001$, $\eta^2 = .570$) and ID ($F(1.69, 28.80) = 34.27$, $p < .001$, $\eta^2 = .668$). Results showed a decrease in the average speed as the task difficulty increased. The interaction between Task and ID was not significant. Pairwise comparisons showed a significantly faster average speed for RW across all IDs (shown in Figure 9 c).

5.7 Subjective Results

NASA-TLX A Wilcoxon signed-rank test revealed a significantly higher workload for BT ($Z = -3.245$, $p < .001$) Figure 10. Further analysis indicated higher mental ($Z = -3.075$, $p < .002$) and physical ($Z = -2.706$, $p < .007$) demands for the BT task, as well as

higher effort ($Z = -3.108$, $p < .002$), and frustration ($Z = -3.467$, $p < .001$) for BT compared to RW.

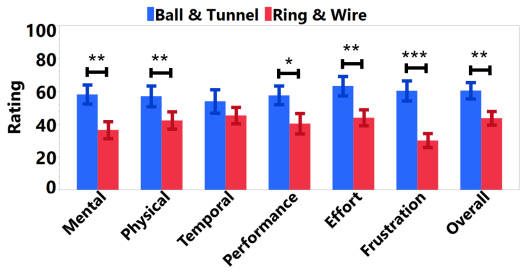

Figure 10: NASA-TLX results. Significance levels are $p < .05$ (*), $p < .01$ (**) and $p < .001$ (***).

SUS A Wilcoxon signed-rank test ($Z = -3.163$, $p < 0.002$) indicated that RW received significantly higher SUS scores (88.47 A-Grade) compared to BT (69.96, B-Grade), indicating that participants found the Ring task more usable.

Post-Experiment Questionnaire 17 participants (94.44%) preferred RW, citing *"better visibility"* (10 mentions), *"greater control"* (7 mentions), and *"more intuitive interaction"* (6 mentions). They found it easier to perceive the ring's boundaries compared to the tunnel, track its position, and adjust their movements accordingly. In contrast, the BT condition was described as *"visually complex"* (7 mentions), making the perception of path boundaries, control, and steering accuracy more difficult, particularly towards the back wall of the tunnel.

6 Discussion

Previous work extended 2D steering into 3D with Ball-and-Tunnel [28] (BT) and Ring-and-Wire [53] (RW). As RW has often been avoided due to its rotational complexity [28, 30, 44], many studies have favored BT [28, 30, 44, 45], which implicitly assumed that the two tasks are interchangeable in 3D mid-air contexts. In this paper, we revisited both tasks in VR and empirically compared their impact on steering performance and user experience.

Our results revealed significant differences between RW and BT in terms of execution metrics (e.g., steering time, average speed, and throughput), traversed path, and subjective ratings (e.g., NASA-TLX and SUS), supporting both our hypotheses. Contrary to common assumptions [28, 30, 44], RW and BT do *not* seem to be interchangeable for studying 3D steering, even when restricted to translational movement, addressing our *RQ1*: are the Ring-and-Wire and Ball-and-Tunnel tasks interchangeable for studying 3D steering when limited to translational movement?

Comparing tasks, participants completed RW faster than BT, with both total and error times consistently lower for RW, indicating that isolated translational movement enables faster steering with reduced cognitive load. As expected per the Steering law [1], path length and width affected task difficulty. Path orientation also significantly influenced steering time, error time, and speed; consistent with prior work [28], these non-linear effects underscore the complexity of 3D steering and highlight the associated motor control challenges [28, 45].

Participants had a higher success rate in BT than with RW, i.e., completed more trials without contacting the boundary, indicating that our modified RW was *not inherently easier*. Although this result does not align with our **H1**, the subjective feedback indicated that participants found BT visually complex and reported difficulty controlling the ball. This suggests that the higher success rate in BT was not due to better boundary perception or intuitiveness. In contrast, participants felt more confident and reported lower cognitive load with RW. RW still showed higher overall performance through faster movements, higher throughput, and more efficient path-following (particularly in narrower widths), supporting **H1**. The added caution in BT also aligns with its higher cognitive load, supporting **H2**. Average speed was consistently higher in RW across all spatial conditions, further supporting this interpretation. Moreover, the total time spent in contact with the boundaries, i.e., the error time, did not significantly differ between tasks. This suggests that although boundary contacts were less frequent in BT, corrective movements were longer, likely due to the tunnel's visual complexity and less precise boundary perception.

Our findings show subtle but important task differences, particularly at narrow path widths where performance diverged. This underscores the role of parameter selection as difficulty increases. At wider widths, deviations grew similarly across tasks, reflecting greater movement variability. Although participants were instructed to steer quickly and accurately rather than follow the centerline, it remains a useful reference as the farthest point from all boundaries. Trajectories often stayed near the center, especially in wider paths and in RW, suggesting clearer boundary perception and fewer corrective movements—consistent with faster performance and lower workload in RW. Movement density further showed that as width increased, steering became more centered in both tasks; at the widest width (0.08 m), movements clustered within smaller central regions, indicating an "effective 3D steering width" analogous to 2D steering [25]. This effect was stronger in RW, where boundaries were clearer. On the frontal plane, tracks consistently shifted backward, more so in BT, likely due to the tunnel's visual complexity and difficulty perceiving the back boundary. Hatira et al. [43] similarly reported that BT users in VR needed to move around the tunnel to identify boundaries. Another potential explanation for the depth shift is the lack of physical support in mid-air interaction [44].

The model-fit results confirm applicability of the Steering law [1] to both tasks, especially for RW, which, to our knowledge, had not been empirically validated in 3D XR contexts. While both tasks showed strong model fits (high R^2 and $Adj.R^2$), throughput differed significantly, with RW yielding higher mean values. This suggests that, despite fitting the Steering law, the tasks are not performance-equivalent. Additionally, aligned with previous work [25, 28, 53], ID significantly affected movement time, error time, and average speed across both tasks. Overall, these results also suggest that RW and BT are not interchangeable, and their results should not be used to build upon.

Through our analysis, we addressed *RQ2*: "What are the key differences between these tasks in the context of 3D mid-air interaction?" Both quantitative and subjective results show that BT imposes a higher cognitive load due to difficulty perceiving tunnel boundaries and limited depth cues, requiring more corrective

actions. In contrast, RW provides clearer visual feedback. These differences have practical implications for selecting tasks in controlled experiments, especially when minimizing perceptual complexity is important. Based on this, we propose the following recommendations for future studies:

The importance of the task type: The Ring-and-Wire and Ball-and-Tunnel tasks are not interchangeable in 3D steering studies, even when rotational movement of the ring is disallowed. Our research focused on spatial characteristics, i.e., width, length, and 3D path orientation, and found that task type significantly influenced the outcomes. Introducing additional factors, e.g., path curvature, distal steering, or alternative interaction techniques, would likely further complicate this effect. Future work should thus carefully choose the task type based on the study's specific goals, especially for higher task difficulties, e.g., narrower paths. Thus, we invite researchers to approach these two tasks separately.

Consider the Ring-and-Wire task as a 3D steering task: The participants exhibited higher performance with RW compared to BT in terms of steering time, throughput, cognitive load, and user preference. RW minimizes perceptual confounds and can provide a more focused measurement of motor control in 3D steering. Besides, given the widespread application of RW in various domains, e.g., fine motor skill training [13, 31, 37], we encourage future research to explore and model the effect of combined rotational and translational movement in RW as a 3D steering task with changing path width, improving the task's representativeness. Our result also questions Liu et al.'s choice on the steering task [28] where the authors used a Ball-and-Tunnel task to limit complexity. Yet our results showed that Ring-and-Wire significantly outperformed Ball-and-Tunnel, with better depth perception, identifying Ring-and-Wire as the less complex one.

The Ball-and-Tunnel task may negatively impact performance in 3D mid-air steering. The visual complexity of the semi-transparent tunnel used in previous research [28–30, 44] can make it more difficult for participants to perceive boundaries, potentially increasing the task difficulty. Researchers and practitioners should be aware that such task properties can introduce perceptual ambiguity or obscure performance differences. The steering performance differences we observed, e.g., the shift in the traversed path in depth, should thus be acknowledged and addressed in the study methodology. Our findings suggest that depth perception near the tunnel's back wall is a critical area, a challenge that has not been addressed in prior work. Future implementations should prioritize depth clarity to overcome the confound of depth misjudgments while steering. Future designs could thus incorporate additional depth cues, e.g., reference grids or geometry [28], leveraging motion parallax and binocular stereo cues by allowing the user's viewpoint to move [19], or modifying the tunnel's material or texture, e.g., overlaying supporting lines [42] or color-to-depth mapping [27]. Beyond visual improvements, providing additional layers of feedback, e.g., auditory and haptic, when the user nears or hits the tunnel boundaries, could also help overcome boundary perception challenges [6, 34, 54, 55]. Such enhancements could reduce unintentional overshoot and improve the reliability of the Ball-and-Tunnel task in steering studies. Moreover, the visual perceptual differences between the tasks suggest the need for further investigation into the perceptual effects on user performance, particularly for more complex tasks, such as curved paths. These additional factors may increase cognitive load and influence research outcomes, highlighting the importance of accounting for task-specific challenges in 3D steering studies. All these are interesting areas for future work.

7 Limitations and Future Work

In our study, ring rotation was constrained, both to isolate translational movement and ensure comparability with BT. Allowing free rotation would transform RW into a dynamic-width steering problem, where the available path width depends on participant-controlled rotation, introducing additional motor demands and potentially higher errors and movement times similar to those observed in previous studies [13, 17, 31]. While beyond the scope of this paper, it highlights the need for future research under more complex conditions, e.g., steering with combined translational and rotational movements, along curvilinear paths, where dynamic width and added motor complexity may alter both modeling requirements and user performance.

Although breaks were provided, cumulative fatigue during long sessions might still affect performance. Still, we found no significant learning effect or performance decline across repetitions ($p > 0.27$ for MT, ET, and TP). Yet, future work, especially with more complex steering tasks, may consider further controlling these effects, e.g., by shortening sessions or distributing trials over different sessions.

Performance variability suggests diverse speed–accuracy strategies, highlighting the need to further study speed–accuracy trade-offs in 3D steering. Besides, path analysis revealed potentially more effective regions, where users avoided boundaries and steered more accurately and faster. As shown in Figure 1(b) and Figure 8, wider paths shifted trajectories toward the center, suggesting possible width thresholds below which 3D steering becomes too difficult. Another critical region was clustering along path boundaries at narrow widths (Figure 1(b) and Figure 8), often in diagonal rather than vertical or horizontal directions. Both effective and critical regions warrant further investigation with broader width ranges and higher-resolution tracking. Finally, examining nonlinear orientation effects alongside these regions could yield deeper insights for improving 3D interaction design.

8 Conclusion

We presented a comparative study of two 3D steering tasks: Ring-and-Wire vs. Ball-and-Tunnel. Our results showed that Ring-and-Wire significantly outperforms Ball-and-Tunnel, with *17.17% faster task execution time, 21.65% higher throughput, and 21.52% higher speed.* Participants also preferred Ring-and-Wire, reporting a lower workload and fewer depth perception issues, particularly with judging the tunnel's backside boundary. These findings revealed that the two tasks are not interchangeable and that task choice critically impacts performance evaluations. We also confirmed the Steering law's applicability for the translational Ring-and-Wire task.

Acknowledgments

We thank the reviewers for their constructive feedback. This work was supported by an NSERC Discovery Grant.

References

[1] Johnny Accot and Shumin Zhai. 1997. Beyond Fitts' law: models for trajectory-based HCI tasks. In *Proceedings of the ACM SIGCHI Conference on Human factors in computing systems*. 295–302.

[2] Johnny Accot and Shumin Zhai. 1999. Performance evaluation of input devices in trajectory-based tasks: an application of the steering law. In *Proceedings of the SIGCHI conference on Human Factors in Computing Systems*. 466–472.

[3] Johnny Accot and Shumin Zhai. 2001. Scale effects in steering law tasks. In *Proceedings of the SIGCHI conference on Human factors in computing systems*. 1–8.

[4] Johnny Accot and Shumin Zhai. 2002. More than dotting the i's—foundations for crossing-based interfaces. In *Proceedings of the SIGCHI conference on Human factors in computing systems*. 73–80.

[5] Mohammadreza Amini, Wolfgang Stuerzlinger, Robert J Teather, and Anil Ufuk Batmaz. 2025. A Systematic Review of Fitts' Law in 3D Extended Reality. In *Proceedings of the CHI Conference on Human Factors in Computing Systems (CHI '25)*.

[6] Oscar Ariza, Gerd Bruder, Nicholas Katzakis, and Frank Steinicke. 2018. Analysis of proximity-based multimodal feedback for 3d selection in immersive virtual environments. In *2018 IEEE Conference on Virtual Reality and 3D User Interfaces (VR)*. IEEE, 327–334.

[7] Cagatay Basdogan, Chih-Hao Ho, Mandayam A Srinivasan, and Mel Slater. 2000. An experimental study on the role of touch in shared virtual environments. *ACM Transactions on Computer-Human Interaction (TOCHI)* 7, 4 (2000), 443–460.

[8] Anil Ufuk Batmaz, Moaaz Hudhud Mughribi, Mine Sarac, Mayra Barrera Machuca, and Wolfgang Stuerzlinger. 2023. Measuring the effect of stereo deficiencies on peripersonal space pointing. In *2023 IEEE conference virtual reality and 3D user interfaces (VR)*. IEEE, 1–11.

[9] Anil Ufuk Batmaz and Wolfgang Stuerzlinger. 2022. Effective Throughput Analysis of Different Task Execution Strategies for Mid-Air Fitts' Tasks in Virtual Reality. *IEEE Transactions on Visualization and Computer Graphics* 28, 11 (2022), 3939–3947. doi:10.1109/TVCG.2022.3203105

[10] Anil Ufuk Batmaz, Xintian Sun, Dogu Taskiran, and Wolfgang Stuerzlinger. 2019. Hitting the wall: Mid-air interaction for eye-hand coordination. In *Proceedings of the 25th ACM Symposium on Virtual Reality Software and Technology*. 1–5.

[11] Anil Ufuk Batmaz, Rumeysa Turkmen, Mine Sarac, Mayra Donaji Barrera Machuca, and Wolfgang Stuerzlinger. 2023. Re-investigating the effect of the vergence-accommodation conflict on 3d pointing. In *Proceedings of the 29th ACM symposium on virtual reality software and technology*. 1–10.

[12] Jennie J.Y. Chen and Sidney S. Fels. 2025. Curves Ahead: Enhancing the Steering Law for Complex Curved Trajectories. In *Proceedings of the CHI Conference on Human Factors in Computing Systems (CHI '25)*. ACM. doi:10.1145/3706598.3713102

[13] Chris G Christou, Despina Michael-Grigoriou, and Dimitris Sokratous. 2018. Virtual buzzwire: Assessment of a prototype VR game for stroke rehabilitation. In *2018 IEEE Conference on Virtual Reality and 3D User Interfaces (VR)*. IEEE, 531–532.

[14] Chris G Christou, Despina Michael-Grigoriou, Dimitris Sokratous, and Marianna Tsiakoulia. 2018. BuzzwireVR: An Immersive Game to Supplement Fine-Motor Movement Therapy.. In *ICAT-EGVE*. 149–156.

[15] Franz Faul, Edgar Erdfelder, Albert-Georg Lang, and Axel Buchner. 2007. G* Power 3: A flexible statistical power analysis program for the social, behavioral, and biomedical sciences. *Behavior research methods* 39, 2 (2007), 175–191.

[16] Paul M Fitts. 1954. The information capacity of the human motor system in controlling the amplitude of movement. *Journal of experimental psychology* 47, 6 (1954), 381.

[17] Mucahit Gemici, Wolfgang Stuerzlinger, and Anil Ufuk Batmaz. 2024. Object Speed Control with a Signed Distance Field for Distant Mid-Air Object Manipulation in Virtual Reality. In *2024 IEEE International Symposium on Mixed and Augmented Reality (ISMAR)*. IEEE, 465–474.

[18] Darren George and Paul Mallery. 2019. *IBM SPSS statistics 26 step by step: A simple guide and reference*. Routledge.

[19] Nicolas Gerig, Johnathan Mayo, Kilian Baur, Frieder Wittmann, Robert Riener, and Peter Wolf. 2018. Missing depth cues in virtual reality limit performance and quality of three dimensional reaching movements. *PLoS one* 13, 1 (2018), e0189275.

[20] Julien Gori, Olivier Rioul, Yves Guiard, and Michel Beaudouin-Lafon. 2018. The perils of confounding factors: How fitts' law experiments can lead to false conclusions. In *Proceedings of the 2018 CHI Conference on Human Factors in Computing Systems*. 1–10.

[21] Jeffrey T Hansberger, Chao Peng, Shannon L Mathis, Vaidyanath Areyur Shanthakumar, Sarah C Meacham, Lizhou Cao, and Victoria R Blakely. 2017. Dispelling the gorilla arm syndrome: the viability of prolonged gesture interactions. In *Virtual, Augmented and Mixed Reality: 9th International Conference, VAMR 2017, Held as Part of HCI International 2017, Vancouver, BC, Canada, July 9-14, 2017, Proceedings 9*. Springer, 505–520.

[22] Sandra G Hart. 2006. NASA-task load index (NASA-TLX); 20 years later. In *Proceedings of the human factors and ergonomics society annual meeting*, Vol. 50. Sage publications Sage CA: Los Angeles, CA, 904–908.

[23] Xuning Hu, Xinan Yan, Yushi Wei, Wenxuan Xu, Yue Li, Yue Liu, and Hai-Ning Liang. 2024. Exploring the effects of spatial constraints and curvature for 3d piloting in virtual environments. In *2024 IEEE International Symposium on Mixed and Augmented Reality (ISMAR)*. IEEE, 505–514.

[24] Patrick W Jordan, Bruce Thomas, Ian Lyall McClelland, and Bernard Weerdmeester. 1996. *Usability evaluation in industry*. CRC press.

[25] Nobuhito Kasahara, Yosuke Oba, Shota Yamanaka, Anil Ufuk Batmaz, Wolfgang Stuerzlinger, and Homei Miyashita. 2024. Better Definition and Calculation of Throughput and Effective Parameters for Steering to Account for Subjective Speed-accuracy Tradeoffs. In *Proceedings of the 2024 CHI Conference on Human Factors in Computing Systems*. 1–18.

[26] Jason Y Lee, Phillip Mucksavage, David C Kerbl, Victor B Huynh, Mohamed Etafy, and Elspeth M McDougall. 2012. Validation study of a virtual reality robotic simulator—role as an assessment tool? *The Journal of urology* 187, 3 (2012), 998–1002.

[27] Zhipeng Li, Yikai Cui, Tianze Zhou, Yu Jiang, Yuntao Wang, Yukang Yan, Michael Nebeling, and Yuanchun Shi. 2022. Color-to-depth mappings as depth cues in virtual reality. In *Proceedings of the 35th annual ACM symposium on user interface software and technology*. 1–14.

[28] Lei Liu, Jean-Bernard Martens, and Robert Van Liere. 2011. Revisiting path steering for 3D manipulation tasks. *international Journal of Human-computer Studies* 69, 3 (2011), 170–181.

[29] Lei Liu and Robert Van Liere. 2012. Modeling object pursuit for desktop virtual reality. *IEEE transactions on visualization and computer graphics* 18, 7 (2012), 1017–1026.

[30] Lei Liu, Robert van Liere, and Krzysztof Jakub Kruszynski. 2011. Modeling the Effect of Force Feedback for 3D Steering Tasks.. In *EGVE/EuroVR*. 31–38.

[31] Lasse F Lui, Unnikrishnan Radhakrishnan, Francesco Chinello, and Konstantinos Koumaditis. 2025. The efficacy of adaptive training in immersive virtual reality for a fine motor skill task. *Virtual Reality* 29, 1 (2025), 20.

[32] Gustavo Luvizutto, Ana Bruno, Sabrina Oliveira, Maristella Silva, and Luciane Souza. 2022. Development and application of an electrical buzz wire to evaluate eye-hand coordination and object control skill in children: a feasibility study. *Human Movement* 23, 2 (2022), 138–144.

[33] I Scott MacKenzie. 2003. Motor behaviour models for human-computer interaction. *HCI models, theories, and frameworks: Toward a multidisciplinary science* (2003), 27–54.

[34] Lawrence Makin, Gareth Barnaby, and Anne Roudaut. 2019. Tactile and kinesthetic feedbacks improve distance perception in virtual reality. In *Proceedings of the 31st Conference on l'Interaction Homme-Machine*. 1–9.

[35] Andrea Mariani, Edoardo Pellegrini, and Elena De Momi. 2021. Skill-Oriented and Performance-Driven Adaptive Curricula for Training in Robot-Assisted Surgery Using Simulators: A Feasibility Study. *IEEE Transactions on Biomedical Engineering* 68, 2 (2021), 685–694. doi:10.1109/TBME.2020.3011867

[36] Robert Pastel. 2006. Measuring the difficulty of steering through corners. In *Proceedings of the SIGCHI conference on Human Factors in computing systems*. 1087–1096.

[37] Unnikrishnan Radhakrishnan, Francesco Chinello, and Konstantinos Koumaditis. 2023. Investigating the effectiveness of immersive VR skill training and its link to physiological arousal. *Virtual Reality* 27, 2 (2023), 1091–1115.

[38] Eric D Ragan, Doug A Bowman, Regis Kopper, Cheryl Stinson, Siroberto Scerbo, and Ryan P McMahan. 2015. Effects of field of view and visual complexity on virtual reality training effectiveness for a visual scanning task. *IEEE transactions on visualization and computer graphics* 21, 7 (2015), 794–807.

[39] F David Rose, Elizabeth A Attree, Bennett M Brooks, David M Parslow, and Paul R Penn. 2000. Training in virtual environments: transfer to real world tasks and equivalence to real task training. *Ergonomics* 43, 4 (2000), 494–511.

[40] Howard W Stoudt. 1973. Arm lengths and arm reaches: Some interrelationships of structural and functional body dimensions. *American Journal of Physical Anthropology* 38, 1 (1973), 151–161.

[41] Ahmed N Sulaiman and Patrick Olivier. 2008. Attribute gates. In *Proceedings of the 21st annual ACM symposium on User interface software and technology*. 57–66.

[42] Haoyu Tan, Tongyu Nie, and Evan Suma Rosenberg. 2024. Invisible Mesh: Effects of X-Ray Vision Metaphors on Depth Perception in Optical-See-Through Augmented Reality. In *2024 IEEE Conference Virtual Reality and 3D User Interfaces (VR)*. IEEE, 376–386.

[43] Laurent Voisard, Amal Hatira, Mine Sarac, Marta Kersten-Oertel, and Anil Ufuk Batmaz. 2023. Effects of Opaque, Transparent and Invisible Hand Visualization Styles on Motor Dexterity in a Virtual Reality Based Purdue Pegboard Test. In *2023 IEEE International Symposium on Mixed and Augmented Reality (ISMAR)*. 723–731. doi:10.1109/ISMAR59233.2023.00087

[44] Yushi Wei, Rongkai Shi, Anil Ufuk Batmaz, Yue Li, Mengjie Huang, Rui Yang, and Hai-Ning Liang. 2024. Evaluating and Modeling the Effect of Frame Rate on Steering Performance in Virtual Reality. *IEEE Transactions on Visualization and Computer Graphics* (2024).

[45] Yushi Wei, Kemu Xu, Yue Li, Lingyun Yu, and Hai-Ning Liang. 2024. Exploring and modeling directional effects on steering behavior in virtual reality. *IEEE*

Transactions on Visualization and Computer Graphics (2024).

[46] Jannik Wiese and Niels Henze. 2023. Predicting Mouse Positions Beyond a System's Latency Can Increase Throughput and User Experience in Linear Steering Tasks. In *Proceedings of Mensch und Computer 2023*. ACM, 101–115.

[47] Jacob O. Wobbrock, Kristen Shinohara, and Alex Jansen. 2011. The effects of task dimensionality, endpoint deviation, throughput calculation, and experiment design on pointing measures and models. In *Proceedings of the SIGCHI Conference on Human Factors in Computing Systems* (Vancouver, BC, Canada) *(CHI '11)*. Association for Computing Machinery, New York, NY, USA, 1639–1648. doi:10.1145/1978942.1979181

[48] Shota Yamanaka and Wolfgang Stuerzlinger. 2024. The Effect of Latency on Movement Time in Path-steering. In *Proceedings of the 2024 CHI Conference on Human Factors in Computing Systems*. 1–19.

[49] Shota Yamanaka, Wolfgang Stuerzlinger, and Homei Miyashita. 2017. Steering through sequential linear path segments. In *Proceedings of the 2017 CHI conference on human factors in computing systems*. 232–243.

[50] Shota Yamanaka, Wolfgang Stuerzlinger, and Homei Miyashita. 2018. Steering through successive objects. In *Proceedings of the 2018 CHI conference on human factors in computing systems*. 1–13.

[51] Shota Yamanaka, Takumi Takaku, Yukina Funazaki, Noboru Seto, and Satoshi Nakamura. 2023. Evaluating the Applicability of GUI-Based Steering Laws to VR Car Driving: A Case of Curved Constrained Paths. *Proceedings of the ACM on Human-Computer Interaction* 7, ISS (2023), 93–113.

[52] Ai-ping Yang, Hui-min Hu, Xin Zhang, Li Ding, and Chau-Kuang Chen. 2021. Natural and forced arm reach ranges in sitting position. *International Journal of Industrial Ergonomics* 86 (2021), 103185.

[53] Shumin Zhai, Johnny Accot, and Rogier Woltjer. 2004. Human action laws in electronic virtual worlds: an empirical study of path steering performance in VR. *Presence* 13, 2 (2004), 113–127.

[54] Yuhang Zhao, Cynthia L Bennett, Hrvoje Benko, Edward Cutrell, Christian Holz, Meredith Ringel Morris, and Mike Sinclair. 2018. Enabling people with visual impairments to navigate virtual reality with a haptic and auditory cane simulation. In *Proceedings of the 2018 CHI conference on human factors in computing systems*. 1–14.

[55] Yuxin Zhao and Zuen Cen. 2024. Exploring Multimodal Feedback Mechanisms for Improving User Interaction in Virtual Reality Environments. *Journal of Industrial Engineering and Applied Science* 2, 6 (2024), 35–41.